Published in final edited form as:
Cancer Res. 2009 January 1; 69(1): 37–44. doi:10.1158/0008-5472.CAN-08-1648.

TGFBI deficiency predisposes mice to spontaneous tumor development

Ye Zhang[1,2], **Gengyun Wen**[1], **Genze Shao**[1,3], **Cuidong Wang**[4], **Chyuansheng Lin**[5], **Hongbo Fang**[2], **Adayabalam S. Balajee**[1], **Govind Bhagat**[6], **Tom K. Hei**[1], and **Yongliang Zhao**[1]

1*Center for Radiological Research, Columbia University, New York, NY 10032*

2*Department of Biochemistry and Molecular Biology, Chinese Academy of Medical Sciences & Peking Union Medical College, Beijing 100005 China*

3*Department of Cancer Biology, University of Pennsylvania, PA 19104*

4*Laboratory of Molecular Biology, The Rockefeller University, New York 10021*

5*Herbert Irving Comprehensive Cancer Center, Columbia University, New York, NY 10032.*

6*Department of Clinical Pathology, Columbia University, New York, NY 10032.*

Abstract

Loss of *TGFBI*, a secreted protein induced by *TGF*-β, has been implicated in cell proliferation, tumor progression and angiogenesis by *in vitro* studies. However, *in vivo* anti-tumor functions of *TGFBI* as well as the underlying molecular mechanism are not well understood. To these aims, we have generated a mouse model with disruption of *TGFBI* genomic locus. Mice lacking *TGFBI* show a retarded growth, and are prone to spontaneous tumors and DMBA (dimethylbenz (a)anthracene)-induced skin tumors. In relative to wild type mouse embryonic fibroblasts (MEFs), $TGFBI^{-/-}$ MEFs display increased frequencies of chromosomal aberration and micronuclei formation, and exhibit an enhanced proliferation and early S-phase entry. *Cyclin D1* is upregulated in $TGFBI^{-/-}$ MEFs, which correlates with aberrant activation of transcription factor CREB (cAMP-response binding protein) identified by chromatin immunoprecipitation (ChIP) and luciferase reporter assays. *TGFBI* reconstitution in $TGFBI^{-/-}$ cells by either retroviral infection with wild type *TGFBI* gene or supplement with recombinant mouse TGFBI protein in the culture medium leads to the suppression of CREB activation and *cyclin D1* expression, and further inhibition of cell proliferation. *Cyclin D1* upregulation was also identified in most of tumors arising from $TGFBI^{-/-}$ mice. Our studies provide the first evidence that *TGFBI* functions as a tumor suppressor *in vivo*.

Introduction

Tumor growth and metastasis is a multistep process involving cell adhesion, proteolytic enzyme degradation of the extracellular matrix (ECM) and motility factors that influence cell migration (1,2). Integrins are cell surface adhesive receptors composed of α- and β-chain heterocomplexes. Both subunits transverse the membrane and mediate the physical and functional interactions between cell and its surrounding ECM, thus serving as bidirectional transducers of extra- and intracellular signals which ultimately lead to regulation of adhesion, proliferation, differentiation, antiapoptosis and tumor progression (3,4).

Correspondence to: Yongliang Zhao or Tom K. Hei, Center for Radiological Research, Columbia University, New York, NY 10032. Email to: E-mail: yz93@columbia.edu or E-mail: tkh1@columbia.edu.
Y. Zhang and G. Wen contributed equally to this work.

TGFBI was first identified in a human lung adenocarcinoma cell line (A549) treated with TGF-β (5). This gene encodes a highly conserved 683 amino-acid protein that contains a secretary signal sequence and four internal homologous domains, the last of which contains an RGD (Arg-Gly-Asp) motif which can serve as a ligand recognition site for integrins (5). TGFBI product has been shown to be a component of ECM in lung and mediate cell adhesion and migration through interacting with integrin via integrin receptors: α3β1, αvβ3, and αvβ5 (6–10). It is ubiquitously expressed in human normal tissues; however, downregulation or lost expression of this gene has been found in a list of human tumor cell lines including lung, breast, colon, prostate, and leukemia as well as in human primary lung and breast tumor specimens (11–14). CpG island hypermethylation in the promoter region, one of the mechanisms by which tumor suppressor genes are inactivated in human cancers, correlates with the silencing of *TGFBI* promoter and its subsequent down-expression (15). *In vitro* studies have implicated its role in maintaining microtubule stability, and inhibiting tumorigenicity and tumor angiogenesis (12,13,16–19), suggesting a tumor suppressor function *in vivo*. To test this hypothesis, we have generated a *TGFBI*-null mouse model. The results demonstrated, for the first time, that *TGFBI* loss promotes cell proliferation through aberrant activation of CREB-*cyclin D1* pathway and predisposes mice to spontaneous tumor development.

Materials and Methods

Generation of *TGFBI* null mice

The *TGFBI* locus was PCR-cloned using a genomic 129 DNA as template. Linearized targeting vector DNA (70 μg) was electroporated into 129Sv/Ev ES cells. Heterozygous targeting ES cells were identified by Southern Blot and two different targeted clones were microinjected into C57BL/6J blastocytes. Chimerical male mice were produced and mated with C57BL/6J females. Germ-line transmission of the targeted *TGFBI* allele was verified by Southern blot analysis of tail DNA from F1 offspring. All mice studied for spontaneous tumor development were the F2 generation of 129Sv/Ev×C57BL/6J crosses. Mice were genotyped by Southern analysis and PCR (primers and conditions available on request). Detailed necropsy and histology are described in the section of Supplementary Information. Protocols were approved by the Animal Care and Use Committee (IACUC) of the Columbia University. Animal procedures were conducted in compliance with IACUC.

Cell cycle analysis

For S-phase re-entry experiment, confluence-arrested cells were plated at 2×10^6 cells per 100 mm dish in medium containing 0.1% serum for 24 h before adding medium containing 10% serum. Following serum stimulation, cells were pulsed with BrdU for one hour at end of the time point and analyzed by FITC-BrdU Flow kit (BD Pharmingen).

Tumor cohorts and carcinogen treatment

For the DMBA-treated cohort, 3–5-day old mice were topically treated with 50 μl of 0.5% DMBA in acetone (Sigma) and monitored for up to 6 months. Mice were visually examined weekly and were killed if any individual tumor reached a diameter of 5 mm, or at the termination of the experiments. Skin tumors will be counted, excised and examined by staining with hematoxylin and eosin.

ChIP analysis

Chromatin Immunoprecipitation (ChIP) assays were carried out as previously described (20), and detected with quantitative PCR (Roter-Gene RG-3000A) (21). Primers for mouse *cyclin D1* gene were 5′-CCGGCTTTGATCTCTGCTTA-3′ (forward) and 5′-CGCGGAGTCTGTAGCTCTCT-3′ (reverse). Primers used for negative control were 5′-

AGGTGGAGAAACACCACCAC-3′ (forward) and 5′- CGGTTTGCCCAAGAAAAATA-3′ (reverse).

Luciferase activity assay and constructs

MEFs were transiently co-transfected with luciferase reporter and dominant negative plasmid. Forty eight hour later, relative luciferase activity was determined by Dural Luciferase Activity Kit (Promega). Relative luciferase activity was normalized to concentration of cell lyates. The relative-fold induction or suppression represents the relative intensity of the experimental sample divided by the relative intensity of the medium control.

RT-PCR method and primers

The expression of *cyclin D1* gene was analyzed by quantitative real-time RT-PCR (Applied Biosystems 7300) using the procedures described previously (14). The primer sets are as following: 5'TCGTGGCCTCTAAGATGAAG3' and 5'TTTTGGAGAGGAAGTGTTCG for mouse *cyclin D1*; 5'AAGGTCATCCCAGAGCTGAA3' and 5'CTGCTTCACCACCTTCTTGA 3' for mouse GAPDH.

To verify the deletion of exons 4–6 in *TGFBI*$^{-/-}$ MEFs, a pair of oligonucleotide primers specific for the upstream and downstream regions of exons 4–6 was designed. The primer sequences: Upstream: 5'CTCATGCGACTGCTGACCCTCGCTCTG(55–81); Downstream: 5'CAGCACACATGGCTGACTTCAGG ATGTG (973–1000)]. cDNAs, synthesized from the total RNAs of WT and *TGFBI*$^{-/-}$ MEFs, were used as the templates for PCR amplification. Using this approach, a 945 bp of PCR product was detected in WT, whereas a 475 bp of PCR product was identified in *TGFBI*$^{-/-}$ MEFs due to the deletion of exons 4–6.

Antibodies and recombinant mouse TGFBI protein

Antibodies used in western blots include mouse monoclonal cyclin D1 (Santa Cruz), rabbit phospho-CREB (ser 133) mAB (Cell Signalings), mouse β-actin mAB (Sigma), anti-CD3 (T cell marker) and anti-CD45R/B220 (B-cell marker) (BD Pharmingen). Rat anti-mouse *TGFBI* mAB and Mouse recombinant TGFBI protein was purchased from R&D systems.

Results

Tumor development in mice lacking *TGFBI* gene

To explore the physiological function of *TGFBI* and its role in tumorigenesis, *TGFBI*-deficient mice were generated by homologous recombination. The correct targeting resulted in the replacement of exons 4–6 of *TGFBI* gene in mice with a neomycin-resistance gene (Fig. 1*A*) and was identified by Southern analysis (Fig. 1*B*). *TGFBI*$^{-/-}$ MEFs still expressed *TGFBI* mRNA but the level was about six-fold lower than in wild type MEFs (data not shown). Moreover, deletion of exons 4–6 in *TGFBI*$^{-/-}$ MEFs was demonstrated by RT-PCR (Fig. 1*C*), and absence of TGFBI protein was revealed by Western blot (Fig. 1*D*).

TGFBI$^{-/-}$ mice arose from crosses of *TGFBI*$^{+/-}$ mice at expected Mendelian frequency and showed a slower postnatal development with a 13.5 ± 3% lower body weight than that of sex-matched *TGFBI*$^{+/+}$ littermates from 2- to 6-month age (n=10) (Supplementary Fig. S1). Histological surveys of liver, lung, kidney, stomach, intestine and testis (n=10 per genotype, age 26 weeks) did not reveal morphological abnormalities. However, 2/10 *TGFBI*$^{-/-}$ mice showed splenomegaly that was identified as B cell hyperplasia (Supplementary Fig. S2).

To assess the tumor-suppressor activity of *TGFBI in vivo*, a large cohort of *TGFBI*$^{-/-}$ (n=54), *TGFBI*$^{+/-}$ (n=75) and *TGFBI*$^{+/+}$ (n=48) animals generated from crosses of *TGFBI*$^{+/-}$ mice were observed for the development of spontaneous malignancies for up to 20 months. Mice

were sacrificed for complete necropsies either at earlier time due to clinical features of systemic illness (weight loss, inactivity, ruffling of fur, and hunched posture) or when reaching end of the observation period. From ages of 9 to16 months, over 20% of *TGFBI*$^{-/-}$ mice died of systemic illness, whereas all *TGFBI*$^{+/+}$ mice were still alive. To determine the cause of death, the moribund *TGFBI*$^{-/-}$ mice between ages of 9 and 16 months were sacrificed and subjected to detailed histopathological analysis. Four out of 12 mice developed malignancies including one invasive lung adenocarcinoma and three lymphomas, one of which was a highly-disseminated lymphoma infiltrating liver and lung tissues (Fig. 2*A*). Others died of unidentified causes with no detectable tumors. Survival of heterozygotes was similar as *TGFBI*$^{+/+}$ mice, and only one died at the end of 16 months without detectable tumor burden. By the end of 20 months, 8.3% (4/48, lung adenocarcinoma and lymphoma) of *TGFBI*$^{+/+}$ mice, 13.3% (10/75, uterus histiocytic sarcoma, hepatocellular carcinoma, lymphoma and lung adenocarcinoma) of heterozygotes, and 37.04% (20/54) of *TGFBI*$^{-/-}$ mice had developed tumors (Fig. 2*B*, Supplementary Table 1, $P<0.01$ for *TGFBI*$^{-/-}$ versus heterozygotes and *TGFBI*$^{+/+}$ mice, χ^2 test). The tumor incidence in heterozygotes is higher than in wild type mice, but didn't reach statistical significance ($P>.05$, χ^2 test). Southern blot-based genotyping analysis showed that the second wild type allele of *TGFBI* gene was retained in all the ten tumors derived from heterozygous mice. However, 3/10 tumors displayed a dense methylation pattern in the *TGFBI* promoter identified by bisulfite sequencing (Supplementary Fig. S3). Tumor-free survival in *TGFBI*$^{-/-}$ mice was significantly lower than in heterozygote and *TGFBI*$^{+/+}$ mice ($P<0.01$, log-rank test, Fig. 2*C*).

An increased skin tumor induction in mice with *TGFBI* deficiency

In skin carcinogenesis assays, we treated *TGFBI*$^{+/+}$, *TGFBI*$^{+/-}$ and *TGFBI*$^{-/-}$ mice with a single dose of DMBA, a chemical carcinogen, on the dorsal skin 3–5 d after birth. The treated mice were checked weekly and monitored for up to six months. Ten of 23 *TGFBI*$^{-/-}$ mice developed skin tumors by 2.5- to 6-month age, two of which formed skin tumors at multiple sites. In contrast, only 2 out of 21 *TGFBI*$^{+/-}$ mice and 1 out of 25 *TGFBI*$^{+/+}$ mice developed tumors during 6-month of observation period. Skin tumor incidence in *TGFBI*$^{-/-}$ mice was significantly higher ($P<0.01$, χ^2 test) than in *TGFBI*$^{+/+}$ and heterozygous mice (Fig. 2*D*). Therefore, mice with *TGFBI* deficiency are prone to the development of both spontaneous malignancies and DMBA-induced skin tumors.

Early passage (P2) of *TGFBI*$^{-/-}$ MEFs exhibits an increased frequency of chromosomal aberrations

To clarify whether disruption of *TGFBI* resulted in an increased frequency of chromosomal aberrations, *TGFBI*$^{-/-}$ and wild type MEFs at passage 2 were treated with 0.05 μg/ml colcemid for 3–6 h. Chromosomal metaphases were prepared from the treated cells, hybridized with cy3-conjugated (C3TA2)3 peptide nucleic acid (PNA) probe (Applied Biosystems) and counterstained with DAPI solution followed the previously reported procedures (22). Digital images were recorded using Zeiss Axioplan 2 microscope with a multicolor image analysis system (Fig. 3*A*). Various types of chromosomal aberrations in *TGFBI*$^{-/-}$ MEFs were shown in Fig. 3*B* (Arrows). Overall, 43.75% (7/17) of metaphases prepared from *TGFBI*$^{-/-}$ MEFs contained chromatid breaks, centric fragments or chromosomal breaks, whereas only 13.3% (2/15) metaphases from wild type MEFs contained only centric fragments (Fig. 3*D*).

In addition, frequency of micronuclei was also examined in the early passage of MEFs (P2). Twenty four hours post plating, cells were fixed with Acetone/ Methanol (1:1) for 10 mins and stained with 0.03 mg/ml acridine orange in dark for 10 mins. A total of 3000 cells were counted for each experiment and three independent assays were performed. Numbers of micronuclei were recorded in each cell type using Nikon Fluorescence microscope. Figure 3C showed multiple micronuclei found in *TGFBI*$^{-/-}$ MEFs (Arrows). Micronuclei frequency in

TGFBI$^{-/-}$ MEFs was 4.7 fold higher than that in wild type MEFs, with 0.128 and 0.027 micronuclei per cell, respectively (Fig. 3*D*).

An accelerated G1-S progression and *cyclin D1* upregulation in *TGFBI*$^{-/-}$ MEFs (passage 18)

To investigate molecular mechanism(s) of tumorigenesis, we characterized mouse embryonic fibroblasts (MEFs) derived from *TGFBI*$^{-/-}$ and *TGFBI*$^{+/+}$ littermates. Long term *in vitro* growth of MEFs was assayed by a 3T3 protocol. *TGFBI*$^{-/-}$ MEFs showed a higher growth at early passage (P2), but grew significantly faster than *TGFBI*$^{+/+}$ MEFs after overcoming the senescence (Fig. 4*A*). This prompted a comparison of the kinetics of S-phase entry in serum-stimulated quiescent cells. Using BrdU incorporation assay, quiescent *TGFBI*$^{-/-}$ MEFs were consistently found to enter into S phase in advance of *TGFBI*$^{+/+}$ MEFs upon serum stimulation (Fig. 4*B*).

We then examined the expression patterns of proteins related to G1-S progression. *Cyclin D1* was identified to be significantly upregulated in *TGFBI*$^{-/-}$ MEFs (Supplementary Fig. S4). Moreover, *cyclin D1* induction was substantially higher in quiescent *TGFBI*$^{-/-}$ MEFs at 4 h post serum stimulation relative to *TGFBI*$^{+/+}$ cells (Fig. 4*C*). However, *TGFBI* reconstitution in *TGFBI*$^{-/-}$ MEFs by infection with retroviral vector containing wild type *TGFBI* gene resulted in a marked suppression of *cyclin D1* expression (Fig. 4*D*) and subsequent inhibition of cell growth measured by BrdU incorporation (Supplementary Fig. S4).

Aberrant activation of CREB and an increased binding activity of p-CREB to *cyclin D1* promoter in the absence of *TGFBI* in *TGFBI*$^{-/-}$ MEFs (Passage 18)

A transcriptional mechanism appears to be involved in *cyclin D1* upregulation since *TGFBI*$^{-/-}$ MEFs showed a 5.6-fold higher level of *cyclin D1* mRNA than wild type cells (Fig. 5*A*). *Cyclin D1* promoter region contains several established or potential binding sites for the transcriptional factors (23). Thus, induction of transcription factors were examined by Western blots in quiescent wild type and *TGFBI*$^{-/-}$ MEFs in response to serum stimulation. Only CREB was identified to be aberrantly activated in *TGFBI*$^{-/-}$ cells (Fig. 5*B*), which is further substantiated by a luciferase reporter assay showing that relative pCRE promoter activity in *TGFBI*$^{-/-}$ cells was over 15-fold higher than wild type cells; however, it can be suppressed significantly by a dominant negative CREB (DN-CREB) vector (Fig. 5*C*, *D*).

To determine whether aberrant activation of CREB in *TGFBI*$^{-/-}$ cells results in an enhanced binding activity of p-CREB to *cyclin D1* promoter, a quantitative PCR-based ChIP assay was used to quantify the bindings of CREB and p-CREB to *cyclin D1* promoter in both wild type and *TGFBI*$^{-/-}$ cells. As shown in Fig. 6*A*, ratio of p-CREB/CREB binding to *cyclin D1* promoter is over five-fold higher in *TGFBI*$^{-/-}$ cells than in wild type cells, suggesting that binding activity of p-CREB to *cyclin D1* is significantly increased in *TGFBI*$^{-/-}$ cells.

TGFBI deficiency correlates with CREB activation and leads to *cyclin D1* upregulation

To determine whether CREB activation is responsible for *cyclin D1* upregulation in *TGFBI*$^{-/-}$ cells (passage 18), a luciferase assay was used to examine the specific suppression of *cyclin D1* promoter activity by dominant negative CREB. The *cyclin D1* promoter activity in *TGFBI*$^{-/-}$ cells was over ten-fold higher than in wild type cells (data not shown); however, it could be inhibited to the similar level of wild type cells by DN-CREB (Fig. 6*B*). This data clearly suggested that CREB activation is involved in *cyclin D1* upregulation in *TGFBI*-null cells.

Correlation between *TGFBI* deficiency and CREB activation was further established by reconstitution of *TGFBI* expression *TGFBI*$^{-/-}$ cells. Compared to wild type cells, *TGFBI*$^{-/-}$ cells showed a significantly higher level of p-CREB and *cyclin D1*, whereas it could be

suppressed to the level of wild type cells after supplement with recombinant mouse TGFBI protein in the culture medium at 0.5 μg/ml for 24 hour (Fig. 6*C*).

Cyclin D1 upregulation in tumors arising from *TGFBI*$^{-/-}$ mice

To define the potential significance of *cyclin D1* upregulation in *in vivo* tumor development, cyclin D1 protein level was examined by Western blotting in tumor tissues arising from *TGFBI*$^{-/-}$ mice. A markedly increased level of cyclin D1 protein was demonstrated in most (10/13) of tumor samples examined in relative to their matched wild type controls (Fig. 6*D*).

Discussion

TGFBI gene has been regionally mapped to chromosome 5q31, a locus often deleted in leukemias, myelodysplastic syndromes and many human cancers such as renal cell, esophageal and lung carcinomas (24–26). In addition, lost expression or downregulation of this gene has been found in a list of human tumor cell lines as well as in primary human lung and breast cancer specimens (11–14). Specifically, *TGFBI* downregulation has been causally linked to an enhanced tumorigenicity and tumor angiogenesis by *in vitro* studies (12,13,18,19). However, it is not clear whether *TGFBI* possesses anti-tumor function *in vivo*. To this aim, *TGFBI*-null mice have been generated. The results showed that mice with *TGFBI* disruption are prone to spontaneous tumors as well as DMBA-induced skin tumors. The most common tumors arising spontaneously in *TGFBI*$^{-/-}$ mice were lymphomas (65.0%, 13/20). Other tumor types were lung papillary adenocarcinoma, skin invasive adenocarcinoma, liver histiocytic sarcoma and testis hemangioendothelioma, which are less common in aged 129Sv/Ev, C56BL/6J mice. Compared with the tumors occurred in *TGFBI*$^{+/+}$ and heterozygous mice, spontaneous tumors arisen from *TGFBI*$^{-/-}$ mice demonstrated metastatic potential: (i) seven out of 13 lymphomas were classified as low grade types with infiltration to other non-lymphoid organs including liver, lung, kidney and pancreas; (ii) four out of 6 other types of tumors were either invasive or metastatic malignancies; (iii) one *TGFBI*$^{-/-}$ mouse developed both invasive lung adenocarcinoma and lymphoproliferative disorder. Hence, *TGFBI* disruption resulted in a dramatic predisposition to lymphomas and other cancers.

Cell cycle progression through the G1 phase requires dual signaling from soluble growth factors and adhesion to the ECM (27). Both RTK (receptor tyrosine kinase)- and intergrin-dependent proliferations are regulated through three major G1-phase targets including induction of *cyclin D1*, and downregulation of the cdk (cyclin–dependent kinases) inhibitors, *p21cip1* and *p27kip1*, which lead to efficient phosphorylation of the retinoblastoma protein (Rb) and progression to S phase (27–29). Under mitogenic conditions, adhesion promotes G1 phase progression primarily via upregulation of *cyclin D1* (30). Since *TGFBI* is an adhesion protein associated with integrin receptor through its RGD motif (8–10), it is expected that an accelerated G1-S transition in *TGFBI*$^{-/-}$ cells is due to the dysregulation of three major G1-phase targets. This is supported by our findings showing that *cyclin D1* is overexpressed in *TGFBI*$^{-/-}$ cells. In contrast, *TGFBI* reconstitution results in a substantially decreased level of *cyclin D1* expression and cellular proliferation. Furthermore, cyclin D1 protein level was demonstrated to be elevated in most of tumors isolated from *TGFBI*$^{-/-}$ mice, suggesting a critical role of *cyclin D1* upregulation in *in vivo* tumor progression in the absence of TGFBI protein. It is well documented that *cyclin D1* plays a major role in controlling G1-S progression, and is consistently upregulated in most human cancers (28,31). Deregulated cell proliferation and increased frequency of spontaneous tumors has been found in transgenic mice with overexpression of *cyclin D1*, whereas deletion of *cyclin D1* protects the mice from tumor induction (32–34). Collectively, these observations together with our findings suggest a critical role of *cyclin D1* upregulation in the enhanced cell proliferation and tumor formation in *TGFBI*$^{-/-}$ mice. However, *cyclin D2*, *cyclin D3*, *cyclin A* and *p21CIP1* expression was not

strongly affected by loss of *TGFBI*, although *p21CIP1* level appeared lower in *TGFBI*$^{-/-}$ MEFs.

CREB has been shown to act as an oncogene and implicated in the development of human endocrine tumors and acute myeloid leukemia (35–37). In this study, CREB was identified to be aberrantly activated after *TGFBI* disruption. In addition, causal links between *TGFBI*-deficiency and CREB activation, and cyclin D1 upregulation have been established in our model system, suggesting that signaling pathway from *TGFBI* to CREB/*cyclin D1* is dysregulated after *TGFBI* disruption, and is involved in tumor progression in *TGFBI*$^{-/-}$ mice. The exact mechanisms of CREB/*cyclin D1* activation downstream of *TGFBI* remain unknown but may include activation of one or more kinases through an integrin-dependent pathway, including FAK, AKT, PKA (Protein kinase A), PKC (protein kinase C), CaMKs (Ca2+/calmodulin-dependent protein kinase), GSK-3 (glycogen synthase kinse III), and CK II (casin kinase II) that have been shown to regulate CREB phosphorylation (35,38). We have found that p-AKT was substantially elevated in serum-starved early passage (P2) of *TGFBI*$^{-/-}$ MEFs at 15min and 30 min post serum stimulation when compared to wild type cells (Supplementary Fig. S5). Previous studies have demonstrated that CREB can be activated by protein kinase B/Akt (38,39), therefore, AKT pathway might mediate *TGFBI*-regulated CREB/*cyclin D1* activation in *TGFBI*$^{-/-}$ cells.

It is commonly accepted that malignant transformation is a lengthy multi-step process and arises through an accumulation of mutations at various genetic loci (40). Genomic instability has been demonstrated to not only initiate tumorigenesis, but is at least a factor in tumor progression (40,41). In the present study, early passage of *TGFBI*$^{-/-}$ MEFs showed a significantly-increased chromosomal aberration and micronuclei than wild type MEFs, suggesting that *TGFBI* deficiency induces genetic instability. This is supported by other study showing that TGFBI protein is involved in microtubule stability and silencing of its expression contributes to centrosome amplification and enhanced mitotic abnormalities (17). It is well documented that chromosomal instability, which is equated to mitotic defects and consequential chromosome segregation errors, provides a formidable basis for the acquisition of further malignant phenotype during tumor progression (42). It should be noted that 3 out of 13 tumor samples isolated from *TGFBI*$^{-/-}$ mice didn't show *cyclin D1* upregulation. Thus, other signaling pathway(s) instead of CREB/*cyclin D1* activation might be aberrantly regulated due to genomic instability.

Although loss of *TGFBI* expression has been found in different types of primary human cancers (11–14), several studies demonstrate that *TGFBI* is commonly overexpressed in colorectal, renal and pancreas cancers (43–45). Also overexpression of *TGFBI* promotes metastasis of SW480 colon cancer cells by enhancing extravasation (45). However, we have found a significant downregulation of *TGFBI* in HT29 colon cancer cells (12). These data clearly point out that dysregulation of *TGFBI* expression is tumor cell or type-specific. It is highly possible that *TGFBI* is a double edged sword whose loss or gain of expression leads to tumorigenesis. Previous studies have shown that *TGFBI* mutations correlate with human corneal dystrophy (46). However, over-expression of mutant TGFBI induces retinal degeneration, but no corneal phenotype was observed in transgenic mice (47). Similarly, we didn't identify any eye phenotypes in *TGFBI*$^{-/-}$ mice.

The present studies provide the evidence, for the first time, that loss of *TGFBI* functions as a tumor suppressor *in vivo*. Because of frequent loss of TGFBI protein in human cancer cells (11–14), *TGFBI* and its associated signaling represent the promising targets for anticancer drug discovery.

Supplementary Material

Refer to Web version on PubMed Central for supplementary material.

Acknowledgements

Grant support: NASA NAG2-1637 (Y. Zhao), CA127120 (Y. Zhao) and NIH ES-11804 (T.K. Hei).

We thank Drs. Ze'ev A. Ronai, Howard B. Lieberman, and Dangsheng Li for critical reading, and Dr. M.R. Montminy (San Diego, CA) for kindly providing WT CREB and dominant negative CREB expression plasmids, and Dr. Isabella Screpanti (University La Sapienza, Rome, Italy) for Mouse *cyclin D1* luciferase reporter plasmid.

References

1. Tlsty TD. Cell-adhesion-dependent influences on genomic instability and carcinogenesis. Curr Opin Cell Biol 1998;10:647–653. [PubMed: 9818176]
2. Giancotti FG, Ruoslahti E. Integrin signaling. Science 1999;285:1028–1032. [PubMed: 10446041]
3. Danen EH. Integrins: regulators of tissue function and cancer progression. Curr Pharm Des 2005;11:881–891. [PubMed: 15777241]
4. Ramsay AG, Marshall JF, Hart IR. Integrin trafficking and its role in cancer metastasis. Cancer Metastasis Rev 2007;26:567–578. [PubMed: 17786537]
5. Skonier J, Neubauer M, Madisen L, Bennett K, Plowman GD, Purchio AF. cDNA cloning and sequence analysis of beta ig-h3, a novel gene induced in a human adenocarcinoma cell line after treatment with transforming growth factor-beta. DNA Cell Biol 1992;11:511–522. [PubMed: 1388724]
6. LeBaron RG, Bezverkov KI, Zimber MP, Pavelec R, Skonier J, Purchio AF. Beta IG-H3, a novel secretory protein inducible by transforming growth factor-beta, is present in normal skin and promotes the adhesion and spreading of dermal fibroblasts in vitro. J Invest Dermatol 1995;104:844–849. [PubMed: 7738366]
7. Billings PC, Herrick DJ, Kucich U, et al. Extracellular matrix and nuclear localization of beta ig-h3 in human bladder smooth muscle and fibroblast cells. J Cell Biochem 2000;79:261–273. [PubMed: 10967553]
8. Kim JE, Jeong HW, Nam JO, et al. Identification of motifs in the fasciclin domains of the transforming growth factor-beta-induced matrix protein betaig-h3 that interact with the alphavbeta5 integrin. J Biol Chem 2002;277:46159–46165. [PubMed: 12270930]
9. Nam JO, Kim JE, Jeong HW, et al. Identification of the alphavbeta3 integrin-interacting motif of betaig-h3 and its anti-angiogenic effect. J Biol Chem 2003;278:25902–25909. [PubMed: 12704192]
10. Jeong HW, Kim IS. TGF-beta1 enhances betaig-h3-mediated keratinocyte cell migration through the alpha3beta1 integrin and PI3K. J Cell Biochem 2004;92:770–780. [PubMed: 15211574]
11. Genini M, Schwalbe P, Scholl FA, Schafer BW. Isolation of genes differentially expressed in human primary myoblasts and embryonal rhabdomyosarcoma. Int J Cancer 1996;66:571–577. [PubMed: 8635876]
12. Zhao YL, Piao CQ, Hei TK. Downregulation of Betaig-h3 gene is causally linked to tumorigenic phenotype in asbestos treated immortalized human bronchial epithelial cells. Oncogene 2002;2:7471–7477. [PubMed: 12386809]
13. Zhao Y, El-Gabry M, Hei TK. Loss of Betaig-h3 protein is frequent in primary lung carcinoma and related to tumorigenic phenotype in lung cancer cells. Mol Carcinog 2006;45:84–92. [PubMed: 16329146]
14. Calaf G, Echiburu-Chau C, Zhao YL, Hei TK. Bigh3 protein expression as a marker for breast cancer. Int J Mol Med 2008;21:561–568. [PubMed: 18425347]
15. Shao G, Berenguer J, Borczuk AC, Powell CA, Hei TK, Zhao Y. Epigenetic inactivation of Betaig-h3 gene in human cancer cells. Cancer Res 2006;66:4566–4573. [PubMed: 16651406]
16. Thapa N, Lee BH, Kim IS. TGFBIp/betaig-h3 protein: a versatile matrix molecule induced by TGF-beta. Int J Biochem Cell Biol 2007;39:2183–2194. [PubMed: 17659994]

17. Ahmed AA, Mills AD, Ibrahim AE, et al. The extracellular matrix protein induces microtubule stabilization and sensitizes ovarian cancers to paclitaxel. Cancer Cell 2007;12:514–527. [PubMed: 18068629]
18. Nam JO, Jeong HW, Lee BH, Park RW, Kim IS. Regulation of tumor angiogenesis by fastatin, the fourth FAS1 domain of betaig-h3, via alphavbeta3 integrin. Cancer Res 2005;65:4153–4161. [PubMed: 15899806]
19. Becker J, Volland S, Noskova I, Schramm A, Schweigerer LL, Wilting J. Keratoepithelin reverts the suppression of tissue factor pathway inhibitor 2 by MYCN in human neuroblastoma: a mechanism to inhibit invasion. Int J Oncol 2008;32:235–240. [PubMed: 18097563]
20. Kuo MH, Allis CD. In vivo cross-linking and immunoprecipitation for studying dynamic Protein:DNA associations in a chromatin environment. Methods 1999;19:425–433. [PubMed: 10579938]
21. Li ZY, Yang J, Gao X, et al. Sequential recruitment of PCAF and BRG1 contributes to myogenin activation in 12-O-tetradecanoylphorbol-13-acetate-induced early differentiation of rhabdomyosarcoma-derived cells. J Biol Chem 2007;282:18872–18878. [PubMed: 17468105]
22. Zijlmans JM, Martens UM, Poon SS, et al. Telomeres in the mouse have large inter-chromosomal variations in the number of T2AG3 repeats. Proc Natl Acad Sci U S A 1997;94:7423–7428. [PubMed: 9207107]
23. Eto I. Molecular cloning and sequence analysis of the promoter region of mouse cyclin D1 gene: implication in phorbol ester-induced tumour promotion. Cell Prolif 2000;33:167–187. [PubMed: 10959625]
24. Peralta RC, Casson AG, Wang RN, Keshavjee S, Redston M, Bapat B. Distinct regions of frequent loss of heterozygosity of chromosome 5p and 5q in human esophageal cancer. Int J Cancer 1998;78:600–605. [PubMed: 9808529]
25. Wu X, Zhao Y, Kemp BL, Amos CI, Siciliano MJ, Spitz MR. Chromosome 5 aberrations and genetic predisposition to lung cancer. Int J Cancer 1998;79:490–493. [PubMed: 9761118]
26. Brezinova J, Zemanova Z, Cermak J, Michalova K. Fluorescence in situ hybridization confirmation of 5q deletions in patients with hematological malignancies. Cancer Genet Cytogenet 2000;117:45–49. [PubMed: 10700866]
27. Assoian RK. Anchorage-dependent cell cycle progression. J Cell Biol 1997;136:1–4. [PubMed: 9026502]
28. Sherr CJ, Roberts JM. CDK inhibitors: positive and negative regulators of G1-phase progression. Genes Dev 1999;13:1501–1512. [PubMed: 10385618]
29. Walker JL, Assoian RK. Integrin-dependent signal transduction regulating cyclin D1 expression and G1 phase cell cycle progression. Cancer Metastasis Rev 2005;24:383–393. [PubMed: 16258726]
30. Welsh CF. Rho GTPases as key transducers of proliferative signals in g1 cell cycle regulation. Breast Cancer Res Treat 2004;84:33–42. [PubMed: 14999152]
31. Hunter T, Pines J. Cyclins and cancer. II: Cyclin D and CDK inhibitors come of age. Cell 1994;79:573–582. [PubMed: 7954824]
32. Wang TC, Cardiff RD, Zukerberg L, Lees E, Arnold A, Schmidt EV. Mammary hyperplasia and carcinoma in MMTV-cyclin D1 transgenic mice. Nature 1994;369:669–671. [PubMed: 8208295]
33. Robles AI, Rodriguez-Puebla ML, Glick AB, et al. Reduced skin tumor development in cyclin D1-deficient mice highlights the oncogenic ras pathway in vivo. Genes Dev 1998;12:2469–2474. [PubMed: 9716400]
34. Yu Q, Geng Y, Sicinski P. Specific protection against breast cancers by cyclin D1 ablation. Nature 2001;411:1017–1021. [PubMed: 11429595]
35. Shaywitz AJ, Greenberg ME. CREB: a stimulus-induced transcription factor activated by a diverse array of extracellular signals. Annu Rev Biochem 1999;68:821–861. [PubMed: 10872467]
36. Rosenberg D, Groussin L, Jullian E, Perlemoine K, Bertagna X, Bertherat J. Role of the PKA-regulated transcription factor CREB in development and tumorigenesis of endocrine tissues. Ann N Y Acad Sci 2002;968:65–74. [PubMed: 12119268]
37. Shankar DB, Cheng JC, Kinjo K, et al. The role of CREB as a proto-oncogene in hematopoiesis and in acute myeloid leukemia. Cancer Cell 2005;7:351–362. [PubMed: 15837624]

38. Delghandi MP, Johannessen M, Moens U. The cAMP signalling pathway activates CREB through PKA, p38 and MSK1 in NIH 3T3 cells. Cell Signal 2005;17:1343–1351. [PubMed: 16125054]

39. Caravatta L, Sancilio S, di Giacomo V, Rana R, Cataldi A, Di Pietro R. PI3-K/Akt-dependent activation of cAMP-response element-binding (CREB) protein in Jurkat T leukemia cells treated with TRAIL. J Cell Physiol 2008;214:192–200. [PubMed: 17579344]

40. Jefford CE, Irminger-Finger I. Mechanisms of chromosome instability in cancers. Crit Rev Oncol Hematol 2006;59:1–14. [PubMed: 16600619]

41. Nowak MA, Komarova NL, Sengupta A, et al. The role of chromosomal instability in tumor initiation. Proc Natl Acad Sci U S A 2002;99:16226–16231. [PubMed: 12446840]

42. Fukasawa K. Oncogenes and tumour suppressors take on centrosomes. Nat Rev Cancer 2007;7:911–924. [PubMed: 18004399]

43. Schneider D, Kleeff J, Berberat PO, et al. Induction and expression of betaig-h3 in pancreatic cancer cells. Biochim Biophys Acta 2002;1588:1–6. [PubMed: 12379307]1.

44. Ivanov SV, Ivanova AV, Salnikow K, Timofeeva O, Subramaniam M, Lerman MI. Two novel VHL targets, TGFBI (BIGH3) and its transactivator KLF10, are up-regulated in renal clear cell carcinoma and other tumors. Biochem Biophys Res Commun 2008;370:536–540. [PubMed: 18359287]

45. Ma C, Rong Y, Radiloff DR, et al. Extracellular matrix protein betaig-h3/TGFBI promotes metastasis of colon cancer by enhancing cell extravasation. Genes Dev 2008;22:308–321. [PubMed: 18245446]

46. Kannabiran C, Klintworth GK. TGFBI gene mutations in corneal dystrophies. Hum Mutat 2006;27:615–625. [PubMed: 16683255]

47. Bustamante M, Tasinato A, Maurer F, et al. Overexpression of a mutant form of TGFBI/BIGH3 induces retinal degeneration in transgenic mice. Mol Vis 2008;14:1129–1137. [PubMed: 18568131]

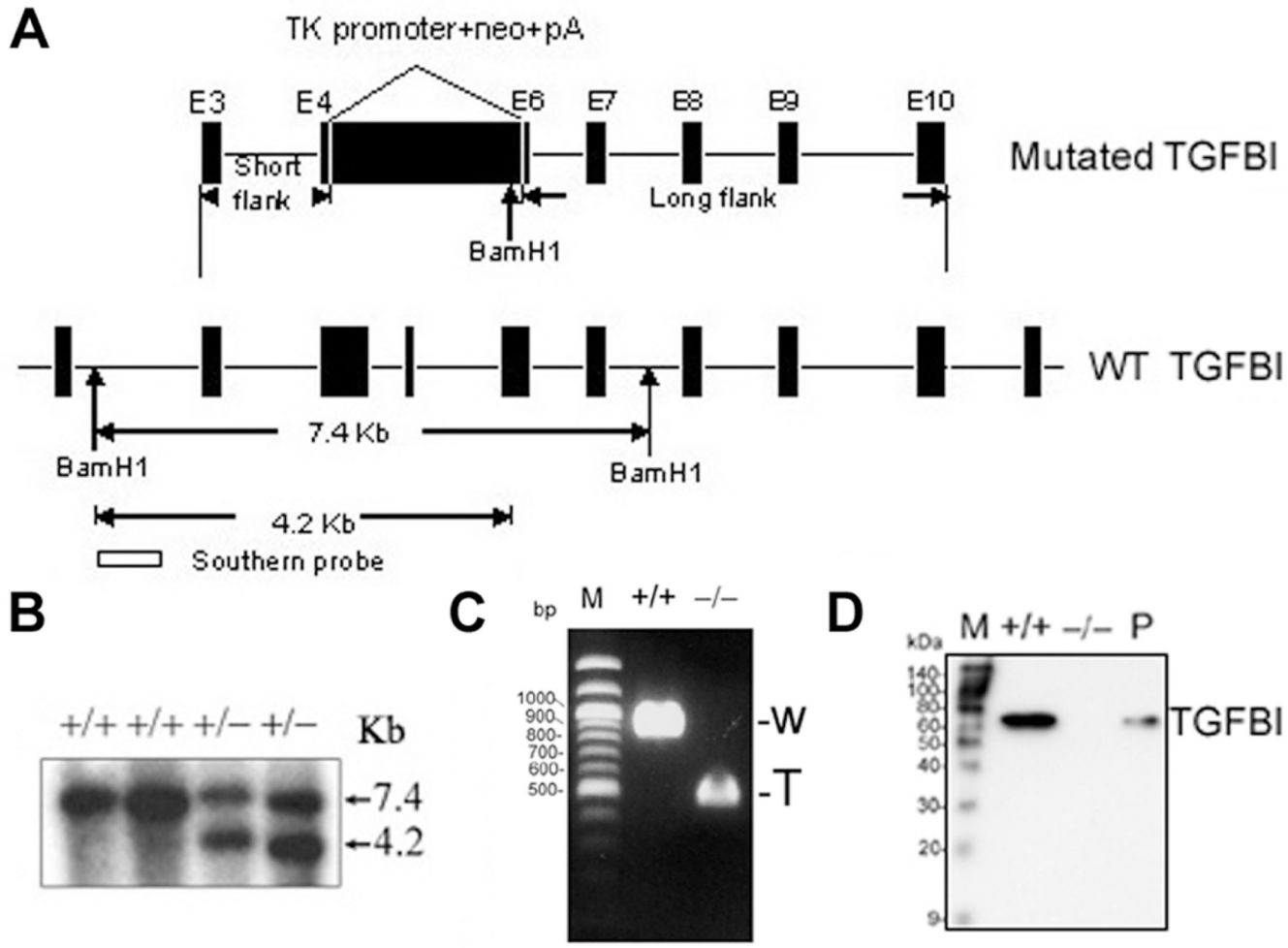

Figure 1. Targeted disruption of *TGFBI* in mice

(A) Strategy for generating the targeted *TGFBI* allele. Exons 4–6 were replaced by neomycin-resistance cassette (neo) with introduction of one BamH1 restriction site at 3' terminal. Targeting construct and wild type allele are shown. Successful targeting will yield a 4.2 kb BamH1-restricted fragment in the neo allele. *(B)* Germinal transmission of the targeted *TGFBI* allele was identified by Southern blot. *(C)* Identification of deletion of exons 4–6 in KO MEFs by RT-PCR using a pair of primers specific for the upstream and downstream regions of exons 4–6. W: wild type; T: truncated. *(D)* Western blot of conditioned medium prepared from MEFs with indicated genotypic backgrounds. Mouse *TGFBI* recombinant protein was used as positive control (P).

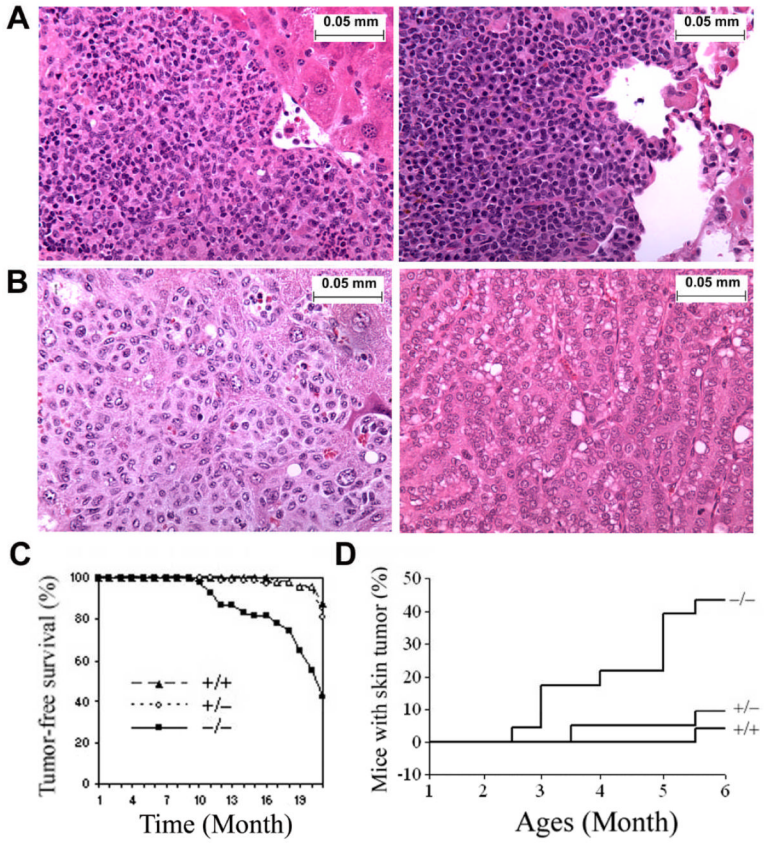

Figure 2. *TGFBI*$^{-/-}$ mice showed an increased tumor incidence

(A) Images of Low grade lymphoma in Live (left panel) and Lung (right panel). *(B)* Image of metastasized tumor in liver (left panel) and lung adenocarcinoma (right panel). Magnification of images (A–B): ×400. *(C)* Tumor-free survival of *TGFBI*$^{-/-}$ mice compared with wild type and heterozygots. *(D)* Incidence of DMBA-induced skin tumors in wild type and *TGFBI*$^{-/-}$ mice.

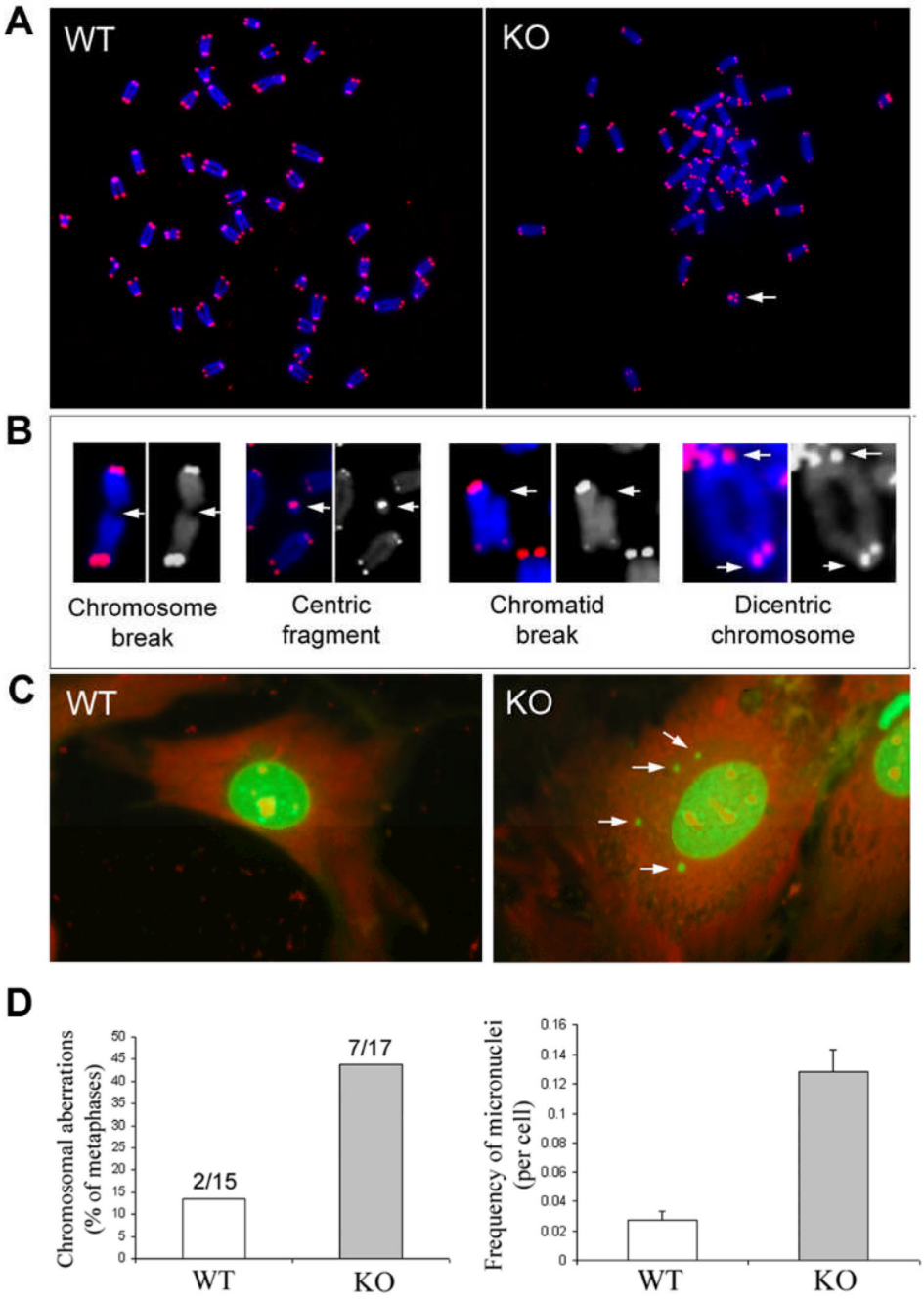

Figure 3. Increased frequency of chromosomal aberrations and micronuclei in early passage (P2) of *TGFBI*$^{-/-}$ MEFs

(A) Digital images of Cy-3 (identify telomeres) and DAPI (identify chromosomes)-stained chromosomal metaphases in wild type and *TGFBI* KO MEFs. Arrow: centric ring. *(B)* Various types of chromosomal aberrations (Arrows) found in KO MEFs. *(C)* Multiple micronuclei (Arrows) identified in KO MEFs. *(D)* Frequency of chromosomal aberrations and micronuclei in wild type and *TGFBI*$^{-/-}$ MEFs.

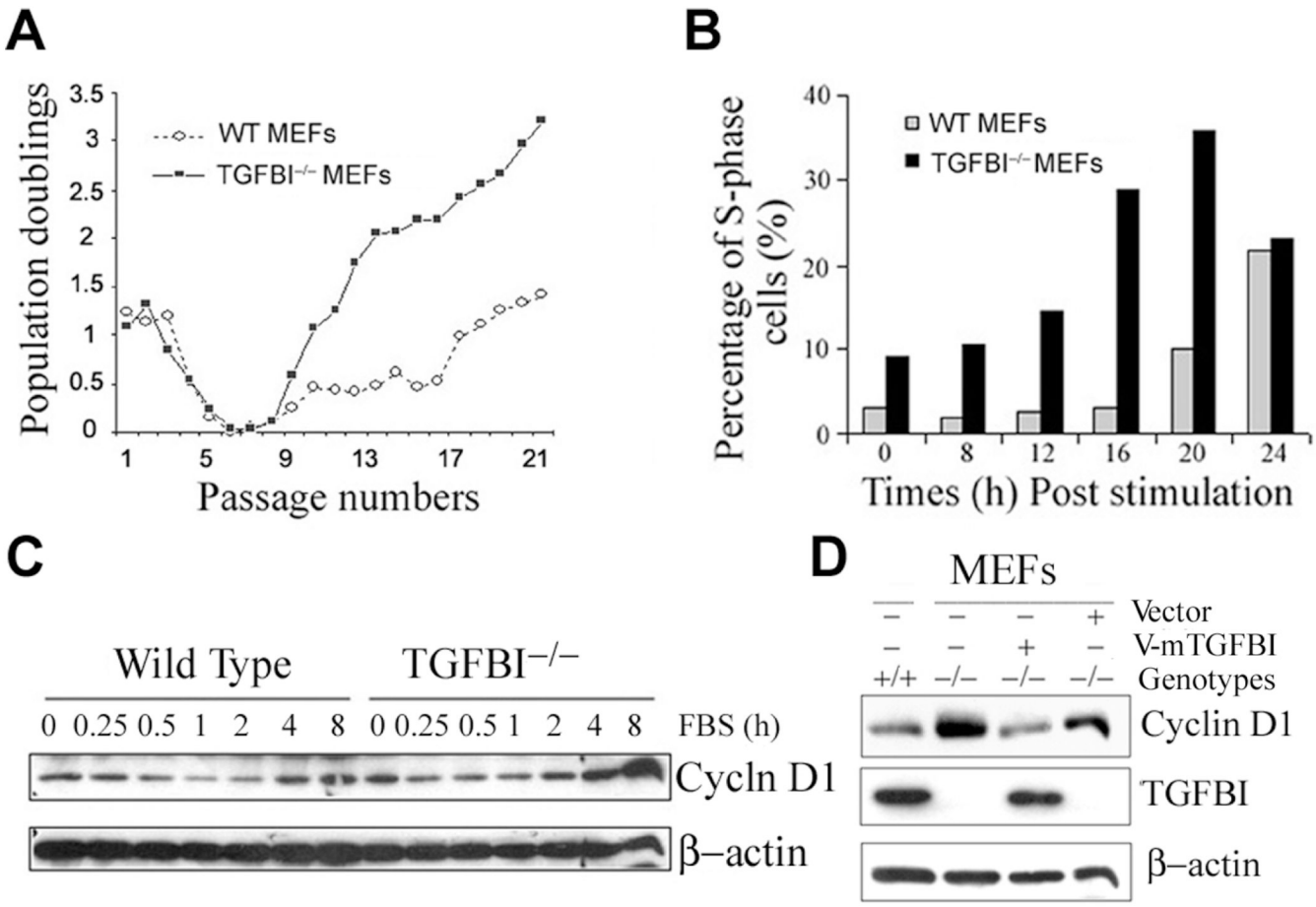

Figure 4. Characterization of growth property and *cyclin D1* expression in *TGFBI*-null MEFs

(A) Cell proliferation on a 3T3 protocol. MEFs were isolated from 13.5-d embryos, and grown at 5% CO_2 in DMEM (Invitrogen) supplemented with 10% FCS. For 3T3 protocol, 9×10^5 cells were plated into 10cm-dish and cell numbers were counted at 3 days interval. At least three independent lines per genotype with two independent cultures per line were examined. *(B)* Kinetics of S-phase entry upon serum stimulation of quiescent *TGFBI*$^{-/-}$ and wild type MEFs. *(C) Cyclin D1* induction in serum-stimulated quiescent *TGFBI*$^{-/-}$ and wild type MEFs determined by Western blots. *(D)* Western blots result of cyclin D1 level in exponentially-grown MEFs with *TGFBI*$^{-/-}$ and wild type backgrounds, and in *TGFBI*$^{-/-}$ MEFs after reconstitution of *TGFBI* by infection with retroviral V-mTGFBI vectors (pMSCV-mTGFBI).

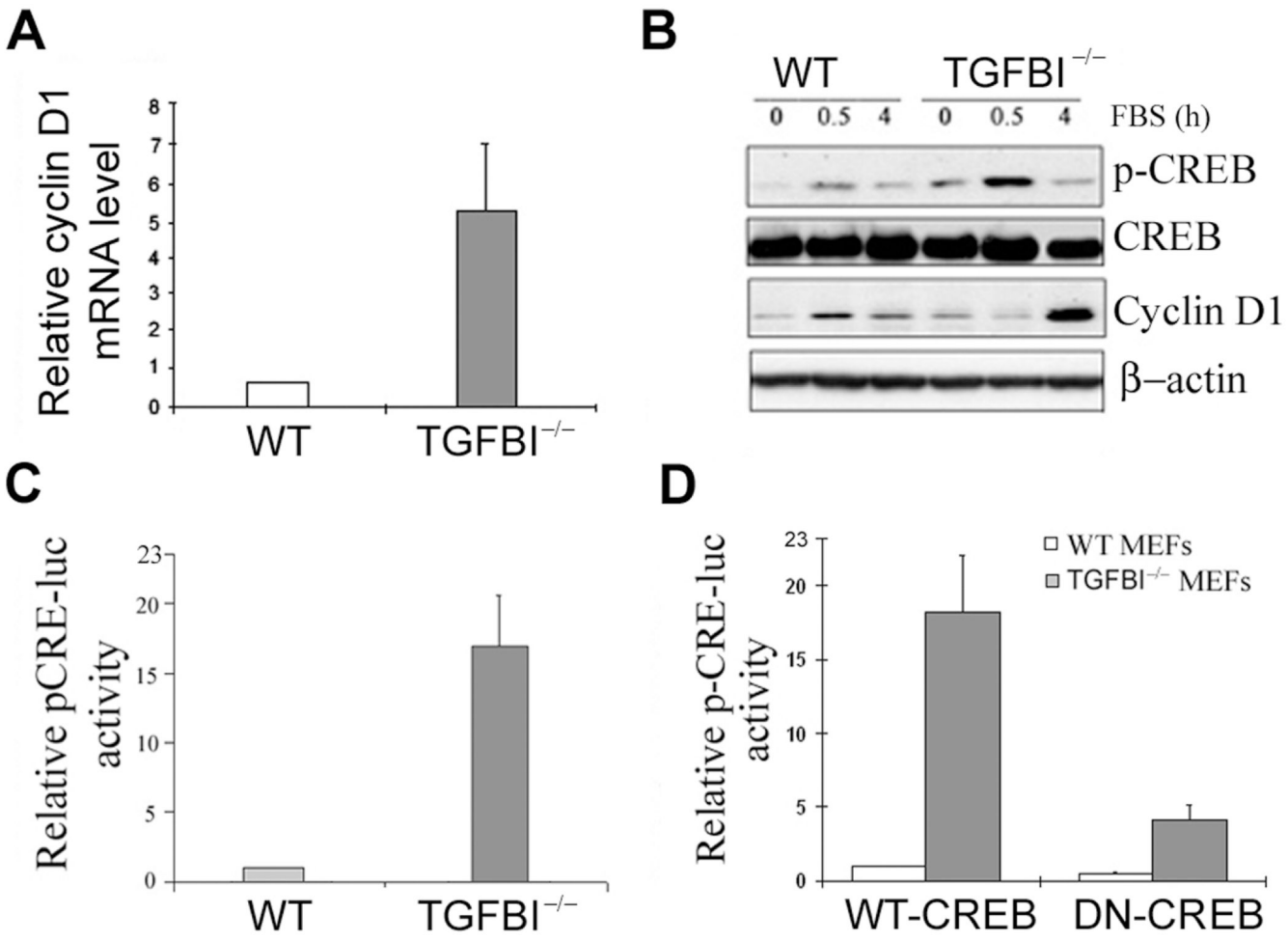

Figure 5. Aberrant activation of CREB in *TGFBI*$^{-/-}$ MEFs

(A) mRNA level of *cyclin D1* in *TGFBI*$^{-/-}$ and wild type MEFs determined by real time RT-PCR. *(B)* Levels of p-CREB and *cyclin D1* in serum-stimulated wild type and *TGFBI*$^{-/-}$ MEFs examined by Western blots. *(C)* Relative pCRE-luc activity in wild type and *TGFBI*$^{-/-}$ MEFs. *(D)* Relative pCRE-luc activity in wild type and *TGFBI*$^{-/-}$ MEFs after co-transfection of pCRE-luc with WT-CREB or DN-CREB vectors.

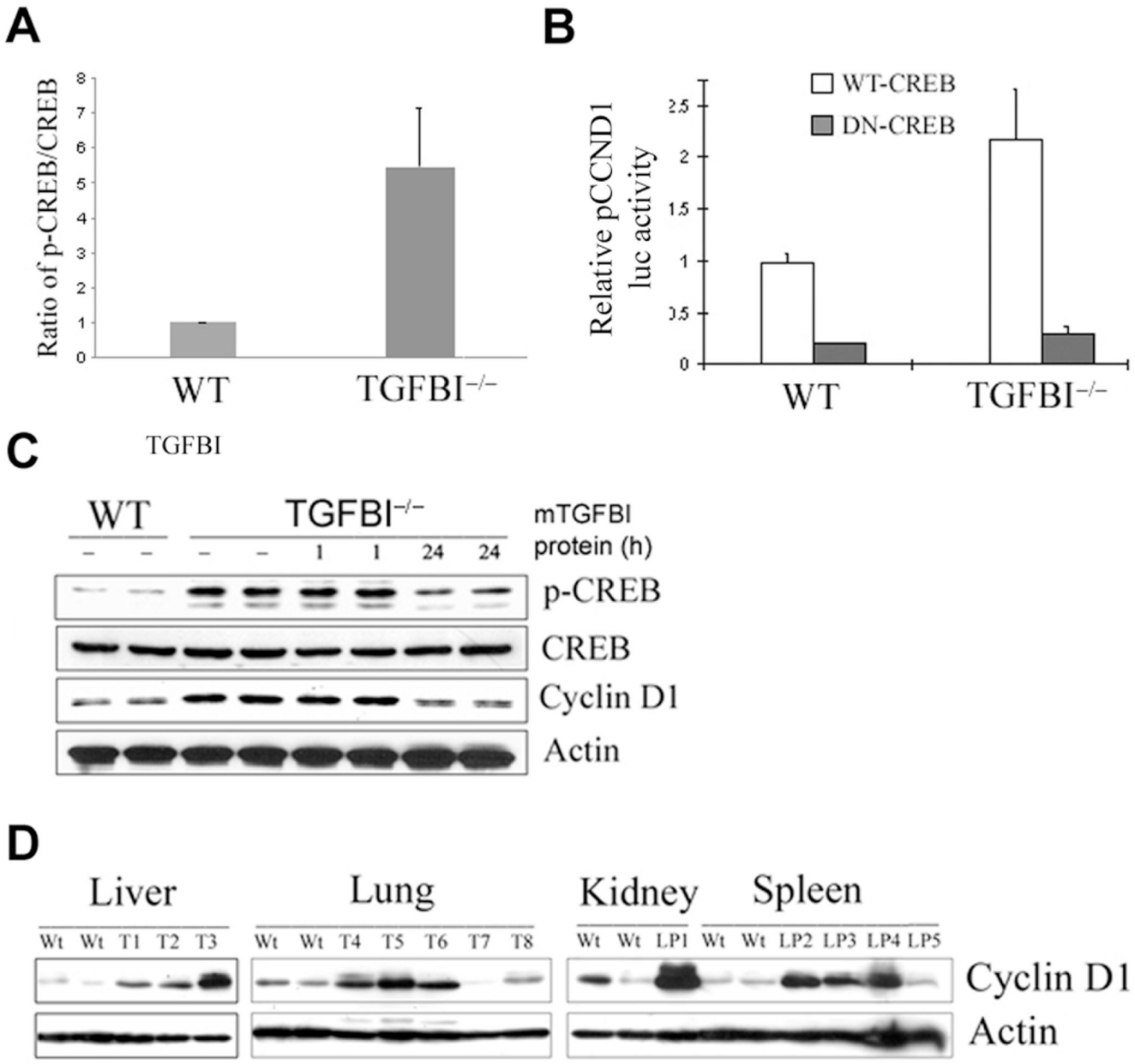

Figure 6. Correlation between CREB activation and *cyclin D1* upregulation in *TGFBI*$^{-/-}$ MEFs

(A) Ratio of pCREB/CREB binding to *cyclin D1* promoter region quantified by a quantitative PCR-based ChIP assay. *(B)* Significant suppression of relative pCCND1 promoter luciferase activity in *TGFBI*$^{-/-}$ MEFs after cotransfection of pCCND1 promoter with wild type CREB or dominant negative CREB vectors. *(C)* Suppression of CREB phosphorylation and *cyclin D1* expression in *TGFBI*$^{-/-}$ cells after incubation with recombinant mouse *TGFBI* protein at 0.5 μg/ml for 24 h. *(D)* Western blot results of cyclin D1 protein level in tumor tissues arising from *TGFBI*$^{-/-}$ mice compared to the tissues from wild type littermates. Wt: wild type; T: tumors; LP: lymphoma.